Bioactive Materials 2 (2017) 71–81

Contents lists available at ScienceDirect

Bioactive Materials

journal homepage: http://www.keaipublishing.com/en/journals/bioactive-materials/

# Human adipose derived stem cells are superior to human osteoblasts (HOB) in bone tissue engineering on a collagen-fibroin-ELR blend

Esen Sayin [a, b], Rosti Hama Rashid [c], José Carlos Rodríguez-Cabello [d], Ahmed Elsheikh [c], Erkan Türker Baran [b], Vasif Hasirci [a, b, e, *]

[a] METU, Department of Biotechnology, Ankara, Turkey
[b] BIOMATEN, METU Center of Excellence in Biomaterials and Tissue Engineering, Dumlupinar Blvd No: 1, 06800 Ankara, Turkey
[c] University of Liverpool, School of Engineering, L69 3GH Liverpool, UK
[d] BIOFORGE, CIBER-BBN, Campus "Miguel Delibes" Edificio LUCIA, Universidad de Valladolid, Paseo Belén 19, 47011 Valladolid, Spain
[e] METU, Department of Biological Sciences, Ankara, 06800, Turkey

ARTICLE INFO

*Article history:*
Received 19 January 2017
Received in revised form
10 April 2017
Accepted 12 April 2017
Available online 27 April 2017

*Keywords:*
Adipose-derived stem cells
Human osteoblasts
Tissue engineering
Bone
Mechanical properties

ABSTRACT

The ultrastructure of the bone provides a unique mechanical strength against compressive, torsional and tensional stresses. An elastin-like recombinamer (ELR) with a nucleation sequence for hydroxyapatite was incorporated into films prepared from a collagen – silk fibroin blend carrying microchannel patterns to stimulate anisotropic osteogenesis. SEM and fluorescence microscopy showed the alignment of adipose-derived stem cells (ADSCs) and the human osteoblasts (HOBs) on the ridges and in the grooves of microchannel patterned collagen-fibroin-ELR blend films. The Young's modulus and the ultimate tensile strength (UTS) of untreated films were 0.58 ± 0.13 MPa and 0.18 ± 0.05 MPa, respectively. After 28 days of cell culture, ADSC seeded film had a Young's modulus of 1.21 ± 0.42 MPa and UTS of 0.32 ± 0.15 MPa which were about 3 fold higher than HOB seeded films. The difference in Young's modulus was statistically significant (p: 0.02). ADSCs attached, proliferated and mineralized better than the HOBs. In the light of these results, ADSCs served as a better cell source than HOBs for bone tissue engineering of collagen-fibroin-ELR based constructs used in this study. We have thus shown the enhancement in the tensile mechanical properties of the bone tissue engineered scaffolds by using ADSCs.



## 1. Introduction

Musculoskeletal disorders are the second biggest reason for long term disability of patients in the world after the mental and behavioral disorders [1]. Fractures or diseases such as osteoporosis lead to a decrease in bone quality and mechanical integrity. Autografts and allografts are used in the conventional therapy of bone defects. Bone autografts are highly preferred over the allografts in order to eliminate infection and immune rejection risks. Availability of vasculature and mechanical properties adequate for cortical bone [2] are important properties of autografts, but their scarcity, site morbidity, infection and bleeding at the extraction site are serious problems. In order to have mechanically strong grafts, ceramics such as hydroxyapatite and tricalcium phosphate [3], which can directly bond to the bone surface, were tested but not preferred because they are brittle and have a high density. Other synthetic options such as bioactive glass [4] were also unsuitable due to their brittleness and tendency to fracture upon cyclic loading or when drilling during implant surgery. On the other hand, bone tissue engineering using synthetic or biological polymers can overcome most of these drawbacks (except mechanical weakness). Besides, degradation products of polyesters such as poly(lactic acid) (PLA) [5], poly(glycolic acid) (PGA) [6] and their copolymers were shown to create an acidic environment. In addition, the synthetic polymers do not possess cell signaling sequences that are naturally present in the structure of biological polymers such as fibronectin, collagen, vitronectin and fibrinogen.

Tissue engineering (TE) can still be an appropriate alternative

* Corresponding author. METU, Department of Biological Sciences, Ankara, Turkey. Tel.: +90 312 2105180.
*E-mail address:* vhasirci@metu.edu.tr (V. Hasirci).
Peer review under responsibility of KeAi Communications Co., Ltd.

http://dx.doi.org/10.1016/j.bioactmat.2017.04.001

for small and medium sized bone defects because TE can introduce to the scaffolds properties like osteoconduction, osteoinduction and osteointegration. The main constituents of bone tissue engineering are biocompatible and biodegradable porous scaffolds and autologous cells to be seeded into the scaffolds to obtain biologically and mechanically adequate tissue substitutes [7]. Recently, protein based scaffolds gained importance in load bearing sites in the body such as bone, cartilage, tendon, meniscus, vessels, skin, bladder and cornea [8], but since they lacked the required mechanical strength, additional materials such as hydroxyapatite for bone needed to be added to improve their mechanical strength [9].

Collagen type I has a special place among the natural polymers because it is secreted by a variety of cells including osteoblasts and constitutes the main organic phase of extracellular matrix (ECM) [10] and contributes significantly to the viscoelasticity of bone [11]. In bone, collagen fibrils are reinforced by plate-shaped HAp nanocrystals 10–20 nm in length and 2–3 nm width [12]. However, reconstituted collagen has a much lower mechanical strength than the bone to be substituted [13]. The reason for this is partly the lack of fibrillar arrangement due to hydrolysis during reconstitution. Additionally, collagen denatures during sterilization and this decreases its resistance to enzymes and mechanical strength [14]. As an alternative to collagen, silk fibroin has been proposed as protein biomaterial for load bearing TE applications due to its unique mechanical properties. Self assembled *Bombyx mori* fibroin molecules have a crystalline β-sheet structure which gives its high tensile strength and toughness, and the remaining amorphous region provides the elasticity needed [15]. However, handling of pure silk fibroin scaffolds is an issue and therefore, it is advantageous to use it as a blend with more flexible materials such as collagen, to achieve optimum mechanical strength and ease of use.

Recently, recombinant proteins have become protein materials of choice due to their tailor-made properties. Elastin-like recombinamers (ELRs) are such recombinant proteins coded in a synthetic DNA and expressed via the use of high yield vectors. VPGXG repeating sequences, where X is a natural or modified amino acid except L-proline originates from elastin which is an ECM protein found in many tissues including bone and is responsible for their elasticity. The amino acid sequences are combined in repeating fashion to form the backbone of ELRs [16]. Most ELRs are thermoresponsive materials and aggregate at temperatures higher than their inverse transition temperature (ITT). This feature aids purification of ELRs via solubilization-precipitation [17]. ELRs have earlier been used in bone tissue engineering and shown to be biocompatible [18]. ELRs with special sequences were reported for bone tissue engineering in order to increase cell adhesion [19], to form an antifouling coat on titanium implants [20] or to enhance nucleation of HAp on the implant surfaces [21].

In this paper, swelling and crystallinity of films of pure collagen, fibroin and their blends were studied. ELR was added to the blend composition to compare the suitability of the stem cells and primary osteoblasts for bone tissue engineering. In this study, an ELR with $[(VPGIG)_2\ (VPGKG)\ (VPGIG)_2]_2$ DDDEEKFLRRIGRFG $[(VPGIG)_2\ (VPGKG)\ (VPGIG)_2]_2$ repeats was used (Fig. 1a). The DDDEEKFLRRIGRFG region is responsible for nucleation of hydroxyapatite. This analog fragment was adapted from statherin, a salivary protein, that has high affinity for calcium and phosphate ions and helps maintain calcification dynamics of tooth enamel [22]. This fragment was shown to induce mineralization on ELR containing surfaces in a supersaturated solution of divalent ions such as simulated body fluid (SBF) [21]. We aimed anisotropic cell growth to mimic the osteon organization. Microchannel pattern decorated films were seeded with human osteoblasts (HOBs) and human adipose-derived stem cells (ADSCs) to align the cells and expected them to secrete ECM in a parallel fashion as in cortical bone. It was hypothesized that alignment could lead to anisotropic mechanical strength to resist the compressive, tensional and torsional forces [23]. In this study the organization of bone lamellae was mimicked with a collagen-fibroin-ELR blend film carrying oriented collagen fibers and the influence of cell type on the mechanical properties of the resultant scaffolds were studied using HOBs and ADSCs (Fig. 1b). This is the first study in the literature that compares mature and stem cells with respect to their proliferation potential and influence on the mechanical strength of the scaffold for their potential use in bone tissue engineering.

## 2. Materials and methods

### 2.1. ELR expression and purification

ELR ($[(VPGIG)_2\ (VPGKG)\ (VPGIG)_2]_2$ DDDEEKFLRRIGRFG $[(VPGIG)_2\ (VPGKG)\ (VPGIG)_2]_2$) carrying an HAp nucleating sequence was produced and characterized by Prof. José Carlos Rodríguez-Cabello (Universidad de Valladolid, Spain). The theoretical mass of the ELR was calculated according to recombinamer design and found as 31,877 Da [24]. Briefly, *E. coli* system was used for the oligopeptide synthesis. Cells were lysed by ultrasonication and protein was purified by applying a series of cold and warm centrifugation steps and dialysis. Purification was carried out by using aggregation of the recombinamer with a lower critical solution temperature (LCST) above its transition temperature. ITT was found to be 32 °C at pH = 7.36 as determined by size measurement between 20 °C and 40 °C by using Nano-ZS (Malvern, Worcestershire, UK). Molecular weight and purity of protein were confirmed by matrix-assisted laser desorption/ionization time-of-flight (MALDI-TOF) with a sharp peak at 31,857.21 Da and sodium dodecyl sulfate polyacrylamide gel electrophoresis (SDS-PAGE) with a distinctive band around 30 kDa that was close to the theoretical mass.

### 2.2. Template preparation

The chemical etching method was applied for the production of patterned silicon wafer at Bilkent University (Ankara, Turkey). Microchannel dimensions were 5 μm, 10 μm, and 5 μm, for ridge width, groove width and depth, respectively (Fig. 1c). Negative replicas were produced from poly(dimethylsiloxane) (PDMS) by mixing PDMS prepolymer and curing agent (Sylgard 184 Elastomer Kit, Dow Corning, Midland, Michigan, USA) in 10:1 ratio and heating at 70 °C for 3 h [25] (Fig. 1d).

### 2.3. Film preparation

Collagen type I was isolated from Sprague–Dawley rat tails and fibroin was purified from silk fibers of *Bombyx mori* according to previously published methods [26]. *Bombyx mori* silk threads were gift from Prof. Esra Karaca, Uludag University (Bursa, Turkey). In brief, for collagen type I isolation, tendons were removed and dissolved in cold acetic acid (0.5 M). Filtered solution was dialyzed against phosphate buffer (24 mM, pH 7.2) and centrifuged. Pellets were dissolved in acetic acid (0.15 M) and NaCl (5%) was added to solution. Next day, precipitated collagen was separated via centrifugation and dissolved in acetic acid (0.15 M). After a week of dialysis, solution was centrifuged and collagen was sterilized in ethanol (70%) for 2 days. Following the centrifugation step, collagen was lyophilized for long term storage. For silk fibroin isolation, silk threads (12.5 g) were washed in boiled $Na_2CO_3$ (0.02 M) for 30 min and dried at 37 °C. Fibroin was dissolved in 9.3 M LiBr (60 °C) and filtered. Solution was dialyzed against water and lyophilized.

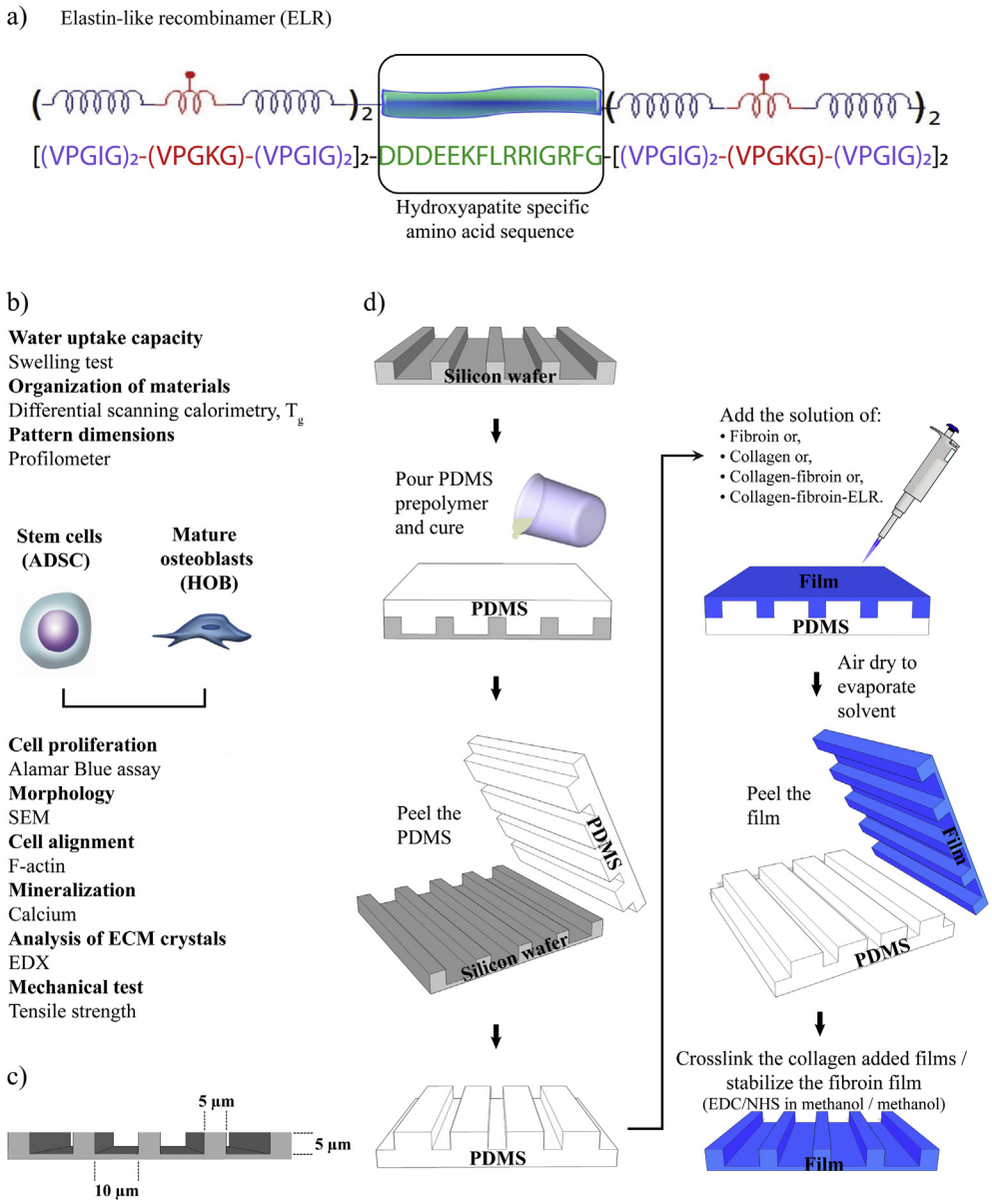


**Fig. 1.** Scheme for the structure of ELR, experimental design and production of pure and blend films. (a) Monomeric structure of the ELR with an amino acid sequence that has affinity to calcium and phosphate. (b) Crosslinked collagen, fibroin and collagen-fibroin blend films were tested for their water uptake capacity and thermal analysis was carried out to find the $T_g$ values of each in order to infer the structural properties of pure materials with respect to their blend. The dimensions of the physical cues were determined before and after the addition of ELR to collagen-fibroin blend that were cast to produce microchannel patterned films. ADSCs and HOBs were seeded on crosslinked collagen-fibroin-ELR films and cultured for 28 days. Surface of the unseeded film and ADSC and HOB films were visualized with SEM to study the effect of polymer degradation and also the cell morphology. Cell guidance was confirmed with cytoskeleton (F-actin) staining. ADSCs and HOBs were tested for their potential to proliferate, mineralize and help for formation of mechanically strong bone tissue substitutes. The Ca/P ratio of the secreted minerals were determined with EDX.

Pure collagen (1.6% (w/v)), pure fibroin (8% (w/v)) and blend of the two (1.6% (w/v) collagen and 0.8% (w/v) fibroin) films were prepared. In order to use for *in vitro* studies, 2.6% (w/v) collagen-fibroin-ELR blend films were produced in a ratio of collagen:fibroin:ELR 6:3:1. For the production of all types of films, materials were dissolved in 0.5 M acetic acid. Solution (250 µL/cm$^2$) was cast on patterned PDMS replicas (2.55 cm$^2$) and dried at room temperature. Afterwards, the collagen bearing films were crosslinked with 1-ethyl-3-[3-dimethylaminopropyl]carbodiimide hydrochloride (EDC) (12.5 mM) and N-hydroxysulfosuccinimide (NHS) (5.2 mM) (Sigma, St. Louis, Missouri, USA) and fibroin films were stabilized in methanol solution (90% v/v) at room temperature as performed at the previous study (Fig. 1d) [26]. After the crosslinking procedure, pattern dimensions (without and with ELR films) were measured with a profilometer (NewView™ 73003D Optical Surface Profiler, Zygo, Middlefield, Connecticut, USA) and compared.

### 2.4. Swelling test

The swelling degrees of pure collagen, pure fibroin and collagen-fibroin blend films were determined via gravimetric method. Pre-weighed, crosslinked films were incubated in 10 mM PBS for 24 h at 37 °C, rinsed with distilled water and blotted lightly. Swelling was calculated as follows:

$$Swelling(\%) = \frac{w_S - w_D}{w_D} \times 100$$

where $w_S$ is the swollen weight and $w_D$ is the dry weight.

### 2.5. Differential scanning calorimetry

Glass transition temperatures of crosslinked collagen, fibroin and collagen-fibroin blend films were determined by differential scanning calorimetry (DSC) (Perkin Elmer Diamond, Waltham, Massachusetts, USA). Samples were heated under nitrogen gas at a rate of 10 °C/min in the range 0–250 °C.

### 2.6. ADSC isolation and characterization

Human fat tissue was obtained from consenting patients at Cag Hospital (Ankara, Turkey) and the project protocols were approved by Middle East Technical University Ethical Committee (B.30.2.ODT.0.AH.00.00/126/95-1585). Lipoaspirate tissue was processed according to the literature [27]. In brief, the tissue was washed with PBS (pH 7.4, 10 mM) and digested with collagenase type I (150 μg/mL, Gibco, Waltham, Massachusetts, USA) in HBSS (Lonza, Basel, Switzerland) on a shaker at 250 rpm for 1 h (37 °C). 10% FBS was added and 160 mM $NH_4Cl$ (pH 7.2) was used to lyse the red blood cells. Bicoll separating solution (Biochrom, Darmstadt, Germany) was used to separate cell layer. Cells were resuspended in PBS and filtered through cell strainers (100 and 40 μm, BD Biosciences, Franklin Lakes, New Jersey, USA). As culture medium, low glucose DMEM (Biochrom, Darmstadt, Germany) supplemented with 40% FBS, 1% penicillin-streptomycin, 250 ng/mL amphotericin B and 10 ng/mL epidermal growth factor (EGF) was used for 1 day. Then floating cells were discarded and FBS ratio was changed to 10%.

For phenotype characterization cells were detached with 0.25% trypsin–EDTA (5 min, at 37 °C) and centrifuged (5 min, 3000 rpm). ADSCs were counted with NucleoCounter (ChemoMetec A/S, Allerod, Denmark). ADSC phenotype was confirmed as reported earlier [26].

### 2.7. HOB isolation and characterization

Bone samples were obtained from the Gulhane Medical Military Academy (GATA) (Ankara, Turkey) with the approval of GATA (50687469-1491-262-14/1648.4-553) and the Middle East Technical University (28620816/203-598) Ethical Committees and consent of the patient. HOBs were isolated from the healthy bone tissue by the surgeon during the elective joint replacement surgery. Bone were cut into pieces and transferred to sterile transport medium (DMEM high glucose supplemented with 2% penicillin-streptomycin, 500 ng/mL amphotericin B). Fragments were placed in medium (DMEM high glucose (Sigma, St. Louis, Missouri, USA) supplemented with 10% FBS, 1% penicillin-streptomycin, 250 ng/mL amphotericin B). After the first week, the medium was refreshed twice a week. Cells migrating out of the explants, reached 90% confluency at the end of 34 days and were trypsinized with 0.25% trypsin–EDTA for 2 min at 37 °C.

For proliferation, harvested cells were transferred into McCoy's 5A (Lonza, Basel, Switzerland) containing 10% FBS, 1% penicillin-streptomycin, 0.5% L-glutamine, 250 ng/mL amphotericin B and 24 μg/mL L-ascorbic acid.

For HOB characterization, the isolated cells were immunostained with anti-collagen type I (Catalog no: ab23446, Abcam, Cambridge, UK) and anti-osteopontin (Catalog no: ab8448, Abcam, Cambridge, UK) antibodies and their nuclei were stained with DAPI (Invitrogen, Waltham, Massachusetts, USA). HOBs were fixed with 4% (w/v) paraformaldehyde for 30 min at room temperature. Cells were washed twice and permeabilized with 1% (v/v) Triton X-100 for 12 min at room temperature. After washing, samples were incubated at 37 °C for 30 min in the blocking solution (1% BSA, 0.1% Tween 20, 0.1% FCS, 0.1% sodium azide in PBS) and samples were incubated with anti-collagen type I and anti-osteopontin antibody solutions (final antibody concentration 10 μg $mL^{-1}$ in 0.1% BSA in PBS) for 2 h at 37 °C. Then, cells were incubated with Alexa Fluor 488-conjugated goat anti-mouse IgG (Catalog no: A11029, Invitrogen, Waltham, Massachusetts, USA) and Alexa Fluor 488-conjugated goat anti-rabbit IgG (Catalog no: A11034, Invitrogen, Waltham, Massachusetts, USA) as secondary antibody (final antibody concentration 20 μg $mL^{-1}$ in 0.1% BSA in PBS) for 1 h at 37 °C to complete the immunostaining of collagen type I and osteopontin markers, respectively. Cell nuclei were stained with DAPI. Samples were visualized with fluorescence microscopy (Zeiss, Jena, Germany). HOBs with passage numbers up to 5 were used in *in vitro* studies.

### 2.8. ADSC and HOB proliferation

Films were sterilized in 70% (v/v) ethanol for 2 h and then air dried inside the laminar flow hood. 10,000 cells were seeded on the films and after one day in growth medium, films were placed into new wells. ADSCs were cultured in the growth medium for 1 week and then the medium was changed with osteogenic medium (high glucose DMEM supplemented with 10% FBS, 1% L-glutamine, 1% penicillin-streptomycin, 250 ng/mL amphotericin B, 100 nM dexamethasone, 10 mM β-glycerophosphate and 50 μM L-ascorbic acid) in which ADSCs were cultured for the next 3 weeks. Since HOBs are originally bone cells no osteogenic medium was used. Proliferation of ADSCs and HOBs were measured with 10% Alamar Blue test (Invitrogen, Waltham, Massachusetts, USA) in colorless DMEM (HyClone, Logan, Utah, USA) on Days 1, 7, 14, 21 and 28. Cells were incubated with Alamar Blue solution for 1 h at 37 °C and optical densities were determined at 570 and 595 nm in a multiwell plate reader (Molecular Devices, Sunnyvale, CA, USA). Absorbances were converted into percent reduction values and cell numbers were determined from a calibration curve.

### 2.9. Scanning electron microscopy (SEM)

Morphologies of ADSCs and HOBs on film surfaces were examined with SEM on Day 28. Additionally, surfaces of unseeded films were examined on Days 1 and 28. Films were washed with PBS and 0.1 M cacodylate buffer (pH 7.4) and then, cells were fixed with glutaraldehyde solution (2.5% in cacodylate buffer) for 2 h at room temperature. Films were stained in 1% osmium tetraoxide (in cacodylate buffer) for 1 h. Samples were dehydrated in graded series of ethanol (50–95%). After final incubation in pure ethanol for 15 min, dehydrated films were freeze dried (Sanyo MDF-U53865, Osaka, Japan), coated with Au-Pd and analyzed with SEM and EDX (FEI, Quanta 400F, Eindhoven, Holland).

### 2.10. Cell alignment

On Day 28, cell seeded samples were stained with Phalloidin Alexa Fluor 532 (Invitrogen, Waltham, Massachusetts, USA). Cells were fixed and permeabilized as explained earlier, incubated in blocking solution (1% BSA in PBS) at 37 °C for 30 min and in Phalloidin solution (118 μg $mL^{-1}$ final concentration prepared in PBS with 0.1% BSA) at 37 °C for 1 h. Images were obtained with Confocal Laser Scanning Microscopy (Zeiss LSM 9100, Lena, Germany).

### 2.11. Mineralization

Quantity of calcium in samples was measured with a colorimetric assay based on o-cresol phthalein complexone that forms a violet colored complex with calcium. Films of Day 28 were washed with PBS and calcium was extracted from them by immersing in 0.6 N HCl overnight at 4 °C. Supernatant (10 μL) was added to a solution (190 μL) containing equal volumes of calcium binding reagent (0.024% o-cresol phthalein complexone and 0.25% 8-hydroxyquinone in water) and calcium buffer (500 mmol/L 2-amino-2-methyl-1,3 propanediol in water). All reagents were purchased from Sigma-Aldrich (St. Louis, Missouri, USA). Absorbance was measured at 570 nm with a multiwell plate reader. The amount of calcium in each sample was determined with a standard curve. Normalized calcium calculations were performed by subtracting the background calcium reading, unseeded film of Day 28, from each value and then dividing with the cell numbers measured with Alamar Blue assay.

### 2.12. Tensile testing of ADSC and HOB seeded films

ADSC and HOB seeded collagen-fibroin-ELR blend films were tested after 28 days of culture to investigate the effect of ECM secretion of cells on the tensile behavior of blend films. None of the samples were fixed. Films ($n = 3–5$) were cut into 4 mm × 10 mm strips and tested at room temperature by Instron 3366 Uniaxial Testing Machine (Instron, Norwood, MA, USA) with a 10 N load cell. Films were placed in a longitudinal direction parallel to the microchannel axis with custom made clamps in a Perspex chamber, which was filled with PBS. Preload (0.01 N) was applied in uniaxial tension mode to prevent loose layout of films between clamps. Preload rate was 0.4 mm/min and no data was recorded during preload. After preload, uniaxial tension was applied up to a maximum load of 10 N at an elongation rate of 0.04 mm/min which corresponded to 1.0%/min strain rate. Testing was continued until failure.

### 2.13. Statistical analysis

Significant differences between groups were examined with one-way ANOVA followed by Tukey's test and $p \leq 0.05$ was taken as statistically significant. Two-way ANOVA was performed for the cell proliferation results. Student's *t*-test was employed for the statistical analysis of the normalized mineralization assay results.

## 3. Results and discussion

### 3.1. Swelling test

ECM is known for its ability to carry water needed for the metabolism [28] and therefore, scaffolds also need to contain a comparable amount of water to create an appropriate microenvironment for the cells. Swelling ratio (water uptake capacity of the films per unit sample weight) was determined for collagen, fibroin and collagen-fibroin blend films. Collagen film gained significantly more water than fibroin film (163% vs 47%) (Fig. 2a and c). It is known that the amorphous regions of the scaffold swell more than crystalline regions due to fewer contact points between the polymeric chains allowing liquid influx [29]. The blend swelled less than the pure collagen film because of the fibroin in the composition of the blend. The presence of collagen twice as much as fibroin led to a significantly higher swelling capacity (139%) than pure fibroin.

### 3.2. Thermal analysis

Glass transition temperature ($T_g$) provides information about the organization of a material. The thermal properties of the collagen and fibroin reported by several studies. Lu et al. found higher $T_g$ value with the increase in the β-sheet structure of the fibroin after stabilization by the use of water annealing process [30]. Additionally, formation of crystalline structure was stimulated by the application of EDC crosslinking to collagen-fibroin blend hydrogels which in turn elevated the $T_g$ of the blend material [31]. DSC revealed that $T_g$ of pure collagen (55.5 °C) was significantly lower than that of pure fibroin (81.5 °C) (Fig. 2b and c) due to the β-sheet rich content of fibroin [32]. The $T_g$ of the blend (58.8 °C) on the other hand is closer to the collagen due to the high collagen content in the blend and much more smaller than fibroin because the crystallinity of fibroin is decreased due to the more amorphous collagen [33]. In the rest of the study, collagen-fibroin-ELR blend was employed since collagen-fibroin blend has superior properties such as optimum water uptake due to collagen and enhanced mechanical strength owing to presence of fibroin.

### 3.3. Pattern dimensions

The depth and width of the grooves and ridges of the microchannels were determined as 4.3 ± 0.1 μm, 10.0 ± 0.3 μm and 7.4 ± 0.3 μm, respectively for the collagen-fibroin blend film by using a profilometer (Fig. 2d). For the ELR-added films, dimensions were 4.6 ± 0.2 μm, 10.3 ± 0.4 μm and 6.8 ± 0.3 μm (Fig. 2e) showing that the presence of ELR does not lead to a distinct change in the dimensions of micropatterns. In addition, both films had the same topography with the template showing the fidelity of the process of microchannel patterned film production.

### 3.4. Characterization of HOB

Human osteoblasts (HOBs) were isolated from the tissues of patients who underwent joint replacement surgery. HOBs were smaller in size in comparison to ADSCs as the phase contrast microscopy images show (Fig. 3a and b). According to literature, HOBs can be half the size of ADSCs but a definite comparison is not possible due to the heterogeneity of the size of ADSCs [34,35]. Additionally, HOB phenotype was confirmed by immunostaining for common human osteoblast markers secreted by HOB: anti-collagen type I for collagen type I and anti-osteopontin for osteopontin [36,37]. These proteins constitute different components of the extracellular matrix in bone. The isolation of HOBs in this study is considered successful because no cells were observed with DAPI-only staining; this indicates that contaminating cells like fibroblasts originating from the isolation step are not present (Fig. 3c and d). Immunostaining also indicated that HOBs preserved their phenotype during passaging up to 5 which was the highest number of passage used in this study.

### 3.5. Proliferation of ADSC and HOB on collagen-fibroin-ELR blend films

Alamar Blue assay was performed to study cell proliferation on Days 1, 7, 14, 21 and 28. The osteogenic differentiation of the ADSCs was induced with the introduction in differentiation medium to drive the ADSCs into osteoblast phenotype. The attachment and proliferation rate of the ADSCs and HOBs were compared for their potential to form an engineered bone tissue on biodegradable films. Collagen-fibroin-ELR blend films supported ADSC adhesion and growth (Fig. 3e). Application of osteogenic medium on Day 7 slowed down the increase in the ADSC proliferation rate and ended

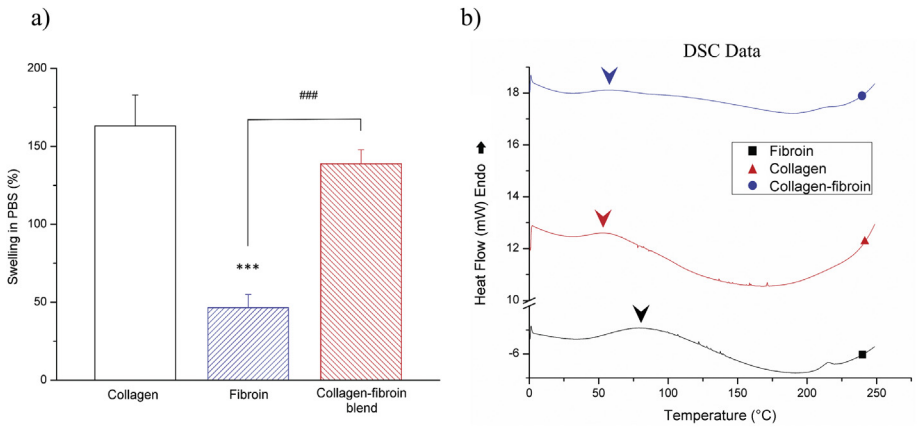


c)

| samples | degree of swelling (%) | $T_g$ (°C) |
|---|---|---|
| **collagen** | 163 | 55.5 |
| **fibroin** | 47 | 81.5 |
| **collagen-fibroin blend** | 139 | 58.8 |

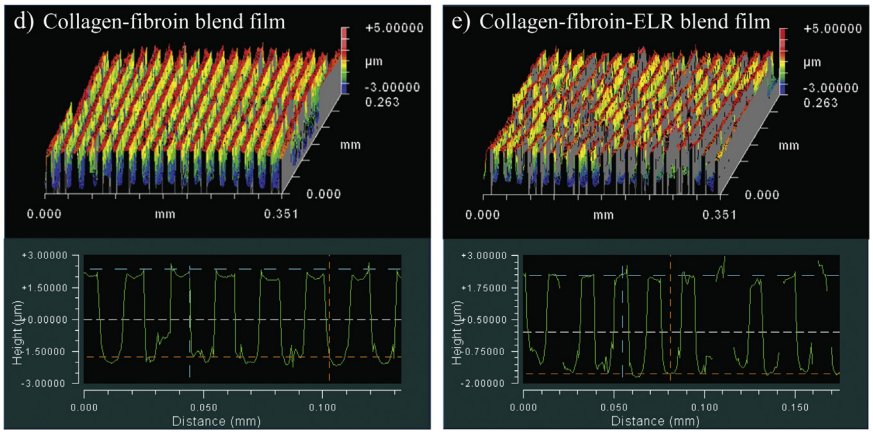


**Fig. 2.** Characterization of pure and blend films. (a) Degree of swelling of collagen, fibroin and collagen-fibroin films. Statistically significant differences were determined between collagen film and other groups ($^{*}p \leq 0.05$, $^{**}p < 0.01$, $^{***}p < 0.001$) and also between fibroin and collagen-fibroin blend films ($^{\#}p \leq 0.05$, $^{\#\#}p < 0.01$, $^{\#\#\#}p < 0.001$). (b) DSC spectra of films. $T_g$ values for each sample are marked with arrows on the DSC spectra. (c) Swelling ratios (%) and $T_g$ of unseeded films. Pattern dimensions of (d) collagen-fibroin, and (e) collagen-fibroin-ELR blend films with microchannel patterns were studied with a profilometer (x20).

in a plateau (on Days 14 and 21) on both TCPS and collagen-fibroin-ELR blend surfaces possibly due to differentiation of stem cells [38]. No osteogenic medium was used for HOBs since they already possessed osteoblast phenotype (Fig. 3c and d) and they showed a proliferation trend as the ADSCs on film. HOBs tested on the same surfaces showed 2-fold lower adhesion on both surfaces than ADSCs (Day 1). As the incubation time went by, the cell number of both HOBs and ADSCs were higher on TCPS (3.9 $cm^2$) than on film (2.55 $cm^2$) surfaces. The larger surface area of the TCPS along with its cell adhesive chemistry can explain the higher cell attachment and proliferation extent. It can be suggested that wider surface of TCPS provided a space for cell attachment and division which in turn might have enhanced Day 1 results of HOBs and ADSCs. Interestingly, number of ADSC on films was approximately 2-fold higher than that of the HOB at each time point. It can therefore be stated that ADSCs proliferate on collagen-fibroin-ELR blend films more than HOBs, despite the low rate due to differentiation. Previously, HOBs were shown to proliferate more on silk fibroin coated PCL - biphasic calcium phosphate (BCP) scaffolds than uncoated ones [39]. Additionally, Gronthos et al. showed that HOBs adhered on the collagen type I surface as well as surfaces coated with other ECM components (collagen types IV, V, fibronectin, laminin, and vitronectin) [40]. According to these studies, HOBs perform well on both collagen and fibroin materials and this is an advantage of the blend film. Similarly, another study pointed out that while ADSCs attached on collagen scaffolds at a higher rate than silk fibroin scaffolds, bone marrow stem cells (BMSCs) attached on both scaffolds without any particular preference for either surface [41].

### *3.6. Surface characterization and morphology of ADSCs and HOBs on collagen-fibroin-ELR blend films*

Collagen-fibroin-ELR blend films patterned with microchannels were produced with predetermined groove and ridge topographies as SEM micrographs showed and crosslinking did not cause any swelling in the physical cues which can be the case in a water based crosslinking medium (Fig. 4a). Features were mainly preserved after crosslinking with EDC/NHS in methanol. Blend films could withstand 27 days of cell culture conditions (Fig. 4b). However, some holes in the films could be seen due to film degradation during culture.

HOBs were lower in number than ADSCs and both HOBs (Fig. 4c)

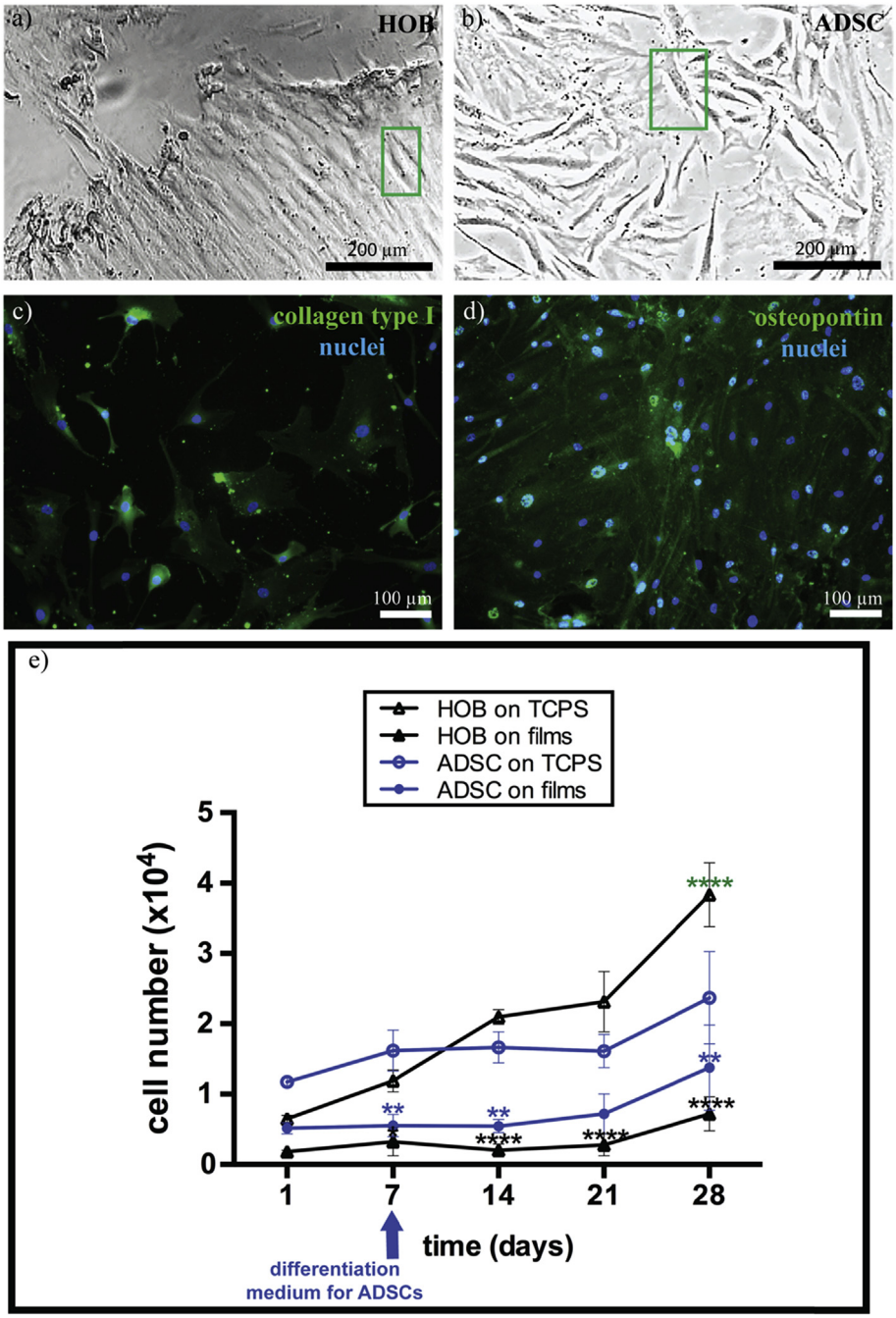


**Fig. 3.** Cell micrographs and proliferation results. Phase contrast images of (a) HOBs and (b) ADSCs. Individual cells were framed with green boxes. Fluorescence micrographs of HOBs isolated from bone tissue and seeded on coverslip. (c) Anti-collagen immunostaining (green). (d) Anti-osteopontin immunostaining (green) (scale bar: 100 µm) (Passage 5). Nuclei were stained with DAPI (blue). (e) HOB and ADSC proliferation on collagen-fibroin-ELR blend films and TCPS control (Alamar Blue assay) (n = 3). On Day 7, osteogenic medium was added for ADSCs. Statistical differences ($^{*}p \leq 0.05$, $^{**}p < 0.01$, $^{***}p < 0.001$, $^{****}p < 0.0001$) were indicated with color codes: black (HOB seeded to TCPS vs film), blue (ADSC seeded to TCPS vs film) and green (HOB seeded vs ADSC seeded TCPS).

and ADSCs (Fig. 4d) were guided on collagen-fibroin-ELR blend film surfaces after 28 days of cell culture. Energy Dispersive X-Ray Spectrometry (EDX) showed no Ca and P atoms on the unseeded (Days 1 and 28) and HOB seeded (Day 28) films. ADSCs, on the other hand, deposited calcium and phosphorus containing compounds on the collagen-fibroin-ELR blend films with a Ca/P ratio of 0.47 after 28 days of cell culture. This value is lower than that of HAp (1.67); its *in vivo* precursor octacalcium phosphate (OCP) has this value as 1.33 [9] and tricalcium phosphate as 1.5. The reason for the 0.47 needs to be further investigated.

### 3.7. ADSC and HOB alignment

Guidance of bone cells is important because it helps an anisotropic ECM deposition by aligned cells. On Day 28, actin filament staining of seeded ADSCs and HOBs showed that cytoskeletons of these cells were aligned along the microchannel direction on patterned collagen-fibroin films (Fig. 5a and b). It can be stated that ADSCs and HOBs were aligned on ridges and grooves smaller than the cells as seen in different examples involving other cell types and materials [43–45]. BMSCs were also a supporting example for cell

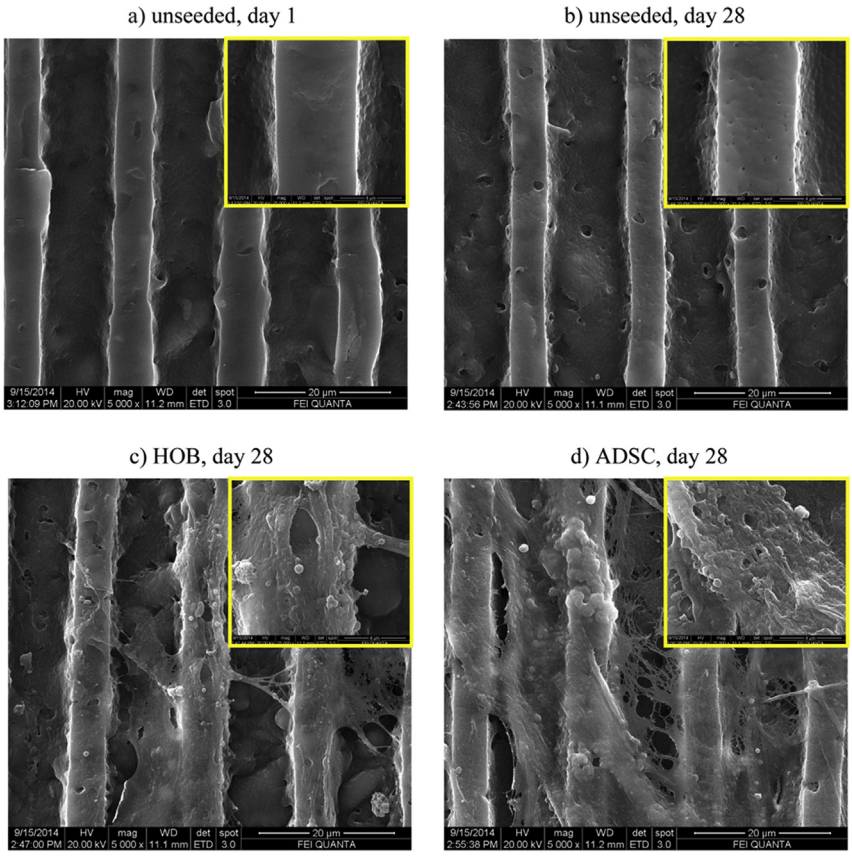


**Fig. 4.** SEM micrographs of unseeded collagen-fibroin-ELR blend films on Days (a) 1, (b) 28 and (c) HOB and (d) ADSC seeded collagen-fibroin-ELR blend films on Day 28. Magnification: ×5,000; ×25,000 (inset).

alignment on a similar sized microchannels composed of thermoresponsive poly(N-isopropylacrylamide) films with ELR adsorbed on the surface [46]. Additionally, the guidance of HOBs was reported by Biggs et al. with the best alignment on microchannels of poly(methylmethacrylate) (PMMA) with the grooves of 10 μm in size amongst the ones that had 25 and 100 μm width [47]. Previously, ADSCs were also reported to align on graphene oxide (ridge: 30 μm, groove: 15 μm) and collagen-fibroin (ridge: 7.4 μm, groove: 10 μm) microchannels with increased osteogenic differentiation in regard to smooth surfaces [26,48].

### 3.8. Quantification of mineralization

The amount of mineral deposited on the HOB and ADSC seeded collagen-fibroin-ELR blend films were quantified with o-cresol phthalein assay on Day 28 in order to get a chemical measurement. Unseeded collagen-fibroin-ELR blend film, incubated for 28 days, was employed as control. Calcium was totally extracted from the film structure via HCl treatment; controls were used for background level check. There was no statistically significant difference between unseeded film of Day 28 (14 μg) and HOB seeded film on Day 28 (24 μg) (Fig. 5c). The low levels of calcium was also supported by EDX analysis. When HOB seeded film was compared with unseeded film on Day 28, it can be said that HOBs deposited calcium however, the amount was not significantly higher. The calcium content of ADSC seeded ELR blend films on Day 28 (274 μg) was significantly higher than on similar films seeded with HOB. Calcium amount was normalized to cell number and ADSCs were shown to deposite significantly higher amounts of mineral than HOBs (Fig. 5d). This result indicated that ADSCs produced more minerals than HOBs.

### 3.9. Mechanical testing

Films that were used in this study were designed to mimic bone lamellae and were tested along the microchannel direction to investigate the contribution of ECM synthesized by the seeded HOBs and ADSCs to the tensile properties. Amruthwar et al. studied the effect of ELR addition to collagen hydrogels for bone tissue engineering. Improvement in the UTS and E were observed from 0.34 MPa to 0.99 MPa and 4.06 MPa to 11.41 MPa with the addition of ELR (25 mg) to collagen (8 mg) hydrogel due to the more concentrated protein content in the scaffold [18]. These values are higher than the UTS and E values measured in this study because of the lower polymer concentration in collagen-fibroin-ELR blend film. Causa et al. reported that addition of 13% (v/v) HAp to PCL scaffolds enhanced the UTS from 0.93 MPa to 2.19 MPa [42]. As far as we know the mechanical properties of bone tissue engineered scaffolds has been enhanced by concentrated solutions of synthetic polymer or with the addition of ceramics. These results in our study showed the importance of seeded cell type on the mechanical strength of bone tissue engineered scaffolds for the first time.

Tensile properties of unseeded collagen-fibroin-ELR blend films on Days 1 and 28 and ADSC and HOB seeded collagen-fibroin-ELR blend films on Day 28 were determined. UTS, E (Fig. 5e) and EB were calculated and the average values are presented in Fig. 5f. No significant difference could be observed for UTS and EB for all groups. On Day 28, unseeded collagen-fibroin-ELR blend film had higher UTS, E and EB than unseeded film on Day 1. This result could be due to collagen degradation being faster than fibroin [26]. This

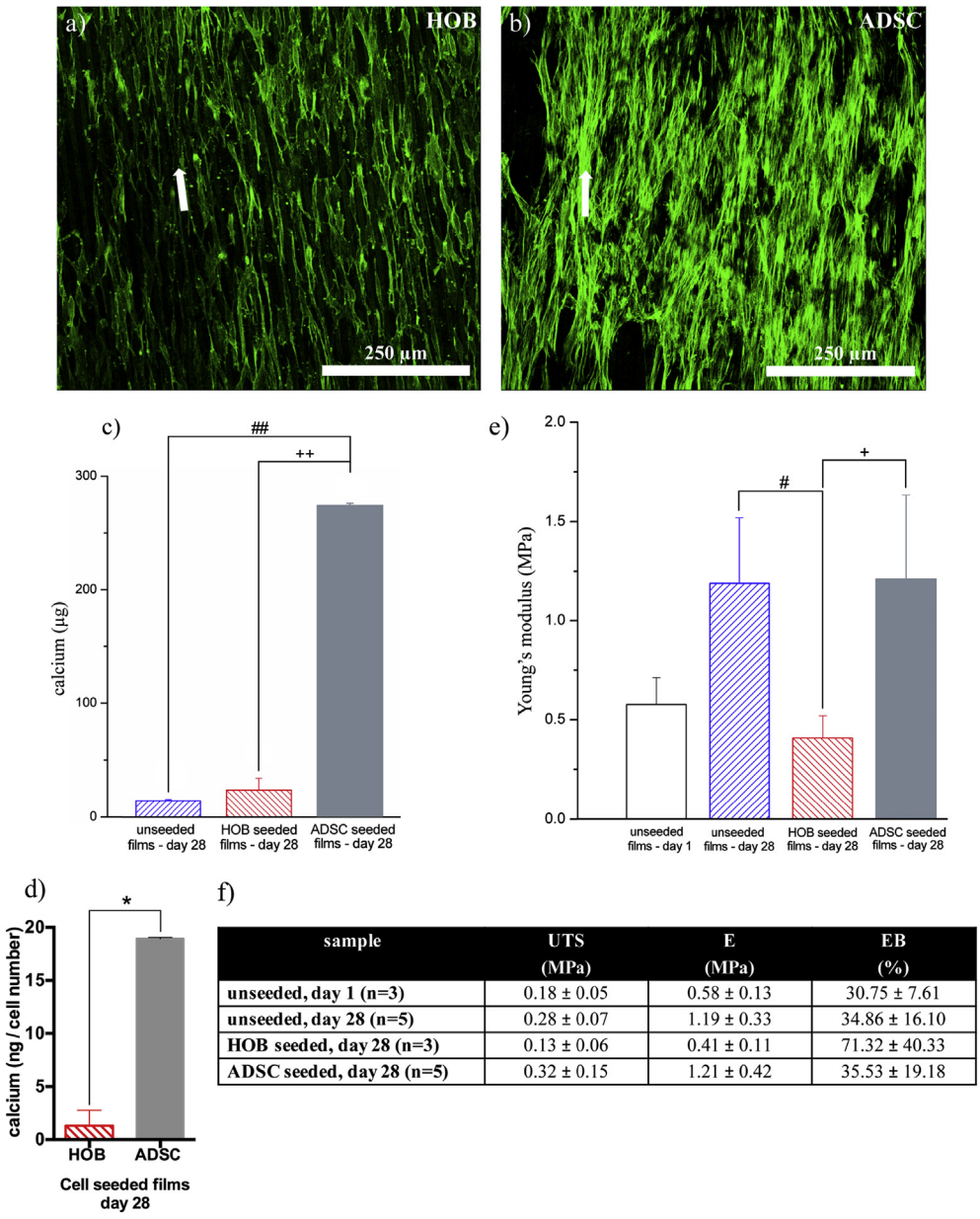


f)

| sample | UTS (MPa) | E (MPa) | EB (%) |
|---|---|---|---|
| unseeded, day 1 (n=3) | 0.18 ± 0.05 | 0.58 ± 0.13 | 30.75 ± 7.61 |
| unseeded, day 28 (n=5) | 0.28 ± 0.07 | 1.19 ± 0.33 | 34.86 ± 16.10 |
| HOB seeded, day 28 (n=3) | 0.13 ± 0.06 | 0.41 ± 0.11 | 71.32 ± 40.33 |
| ADSC seeded, day 28 (n=5) | 0.32 ± 0.15 | 1.21 ± 0.42 | 35.53 ± 19.18 |

**Fig. 5.** HOBs and ADSCs were tested for their ability to align, deposit calcium minerals and contribute to tensile properties. Fluorescence micrographs of actin filament stained with Phalloidin (green) on Day 28 shows the cell alignment along the microchannel direction (white arrow). (a) HOB and (b) ADSC on collagen-fibroin-ELR blend films (scale bar: 250 µm). (c) Calcium amounts of unseeded collagen-fibroin-ELR blend films, HOB and ADSC seeded collagen-fibroin-ELR blend films were quantified by o-cresol phthalein complexone method on Day 28. Statistical differences were determined and differences between the groups were analyzed. (d) Calcium amounts of HOB and ADSC seeded films were normalized to cell number. (e) Young's modulus of the unseeded and seeded films are presented with the statistical analysis (*$p \leq 0.05$, **$p < 0.01$; *: unseeded film on Day 1 vs other groups, #: unseeded film on Day 28 vs HOB and ADSC seeded films on Day 28, +: HOB vs ADSC seeded films on Day 28). (f) The average ultimate tensile strength (UTS), Young's modulus (E) and elongation at break (EB) values of unseeded and seeded collagen-fibroin-ELR blend films (n = 3–5).

selective degradation could expose a stronger and crystalline structure of fibroin (β-sheet) after 28 days of cell culture. The higher β-sheet level of fibroin was supported by its low swelling degree and high $T_g$ which are indications of the superior crystallinity of fibroin over collagen film. Similar to our results, the positive relationship between higher crystallinity level of more crosslinked polycaprolactone fumarate and increased tensile modulus was reported by another study [49]. Hu et al. employed films formulated with recombinant human like collagen and fibroin for hepatic tissue engineering purposes. They showed EB elevated from 28.7% to 30.9% with the increase of fibroin content by 10% (w/w) in films [50]. In our work, on Day 1, E was 0.58 ± 0.13 MPa for unseeded collagen-fibroin-ELR blend film. This value is higher than the literature value of 502 ± 575 kPa which was measured from crosslinked and microchannel patterned HAp nucleated ELR membrane after 7 days of incubation in simulated body fluid [51]. By taking this result into account, it can be suggested that collagen and fibroin promoted the mechanical strength of the film.

ADSC seeding contributed to the UTS and E which indicated ECM secretion however, HOB seeding decreased these properties substantially and led to highest EB. Significantly enhanced E in ADSC seeded film (1.21 MPa) when compared to HOB seeded film (0.41 MPa) could be explained by matrix metalloproteinase-2 (MMP-2) secretion, by HOBs *in vitro* [52]. A relevant work also

showed that MMP-2 is downregulated during osteogenic differentiation of ADSCs [53] and therefore, degradation by MMP-2 might have lowered E significantly for HOB seeded film by breaking the protein chains and leaving them more stretchable. In return, this effect could lead to increase in the EB up to 2-fold (71.32%) when compared to other films. Additionally, Ascenzi et al. applied tensile test in longitudinal direction for wet human fully calcified osteon and measured EB as 6.84% [54] which is five-fold lower than that of Day 28 film on which ADSCs were seeded (35.53 ± 19.18%).

## 4. Conclusions

In this study, swelling test and DSC experiments showed that the reason of higher mechanical strength of unseeded film incubated for 28 days when compared to Day 1 film was the increase in fibroin fraction relative to collagen as a result of the polymer degradation. Guided HOBs and ADSCs on microchannel patterned collagen-fibroin-ELR blend films mimicked the naturally aligned bone tissue. Furthermore, higher rates of cell adhesion, proliferation, mineralization and mechanical properties were obtained by ADSC seeding when compared to HOB due to enhanced ECM secretion. Potential of ADSC over HOB was proven by these means are vital for bone tissue engineering substrates. Osteogenically differentiated ADSCs improved the stiffness and tensile strength of the collagen-fibroin-ELR films after 28 days of incubation.

## Conflict of interests

We declare that authors have no competing financial interest.

## Acknowledgements

We acknowledge Prof. Muharrem Demirogullari from Cag Hospital (Ankara, Turkey) and Prof. Cemil Yildiz from GATA (Ankara, Turkey) for providing the lipoaspirate material and bone sections, respectively. We would like to acknowledge Prof. Esra Karaca from Uludag University (Bursa, Turkey) for kindly providing the *Bombyx mori* silk threads. We would like to acknowledge METU Central Laboratory for DSC and SEM analysis. The authors would like to thank METU (BAP-07.02.2013.101) for the financial support of the study by E.S., and the Scientific and Technological Research Council of Turkey (TUBITAK) for the scholarship to E.S. through BIDEB 2211C. We are grateful to Ministry of Development of Turkey for funding BIOMATEN through Grant DPT2011K120350. J.C.R.C. acknowledges the funding from the EC (HEALTH-F4-2011-278557, PITN-GA-2012-317306, MSCA-ITN-2014-642687 and NMP-2014-646075), MINECO (MAT2013-42473-R and MAT2015-68901R) and JCyL (VA244U13, VA313U14 and VA015U16).

## References

[1] T. Vos, et al., Years lived with disability (YLDs) for 1160 sequelae of 289 diseases and injuries 1990-2010: a systematic analysis for the Global Burden of Disease Study 2010, Lancet 380 (2012) 2163–2196, http://dx.doi.org/10.1016/S0140-6736(12)61729-2.

[2] P.V. Giannoudis, H. Dinopoulos, E. Tsiridis, Bone substitutes: an update, Injury 36 (Suppl 3) (2005) S20–S27, http://dx.doi.org/10.1016/j.injury.2005.07.029.

[3] S. Tarafder, V.K. Balla, N.M. Davies, A. Bandyopadhyay, S. Bose, Microwave-sintered 3D printed tricalcium phosphate scaffolds for bone tissue engineering, J. Tissue Eng. Regen. Med. 7 (2013) 631–641, http://dx.doi.org/10.1002/term.555.

[4] M.N. Rahaman, D.E. Day, B. Sonny Bal, Q. Fu, S.B. Jung, L.F. Bonewald, A.P. Tomsia, Bioactive glass in tissue engineering, Acta Biomater. 7 (2011) 2355–2373, http://dx.doi.org/10.1016/j.actbio.2011.03.016.

[5] A.S. Badami, M.R. Kreke, M.S. Thompson, J.S. Riffle, A.S. Goldstein, Effect of fiber diameter on spreading, proliferation, and differentiation of osteoblastic cells on electrospun poly(lactic acid) substrates, Biomaterials 27 (2006) 596–606, http://dx.doi.org/10.1016/j.biomaterials.2005.05.084.

[6] E.D. Boland, G.E. Wnek, D.G. Simpson, K.J. Pawlowski, G.L. Bowlin, Tailoring tissue engineering scaffolds using electrostatic processing techniques: a study of poly(glycolic acid), J. Macromol. Sci. Part A 38 (2001) 1231–1243, http://dx.doi.org/10.1081/MA-100108380.

[7] I. Rajzer, E. Menaszek, R. Kwiatkowski, J.A. Planell, O. Castano, Electrospun gelatin/poly(ε-caprolactone) fibrous scaffold modified with calcium phosphate for bone tissue engineering, Mater. Sci. Eng. C 44 (2014) 183–190, http://dx.doi.org/10.1016/j.msec.2014.08.017.

[8] E. Sayin, E.T. Baran, V. Hasirci, Protein-based materials in load-bearing tissue-engineering applications, Regen. Med. 9 (2014) 687–701, http://dx.doi.org/10.2217/rme.14.52.

[9] M.T. Arafat, C.X.F. Lam, A.K. Ekaputra, S.Y. Wong, X. Li, I. Gibson, Biomimetic composite coating on rapid prototyped scaffolds for bone tissue engineering, Acta Biomater. 7 (2011) 809–820, http://dx.doi.org/10.1016/j.actbio.2010.09.010.

[10] R. Murugan, S. Ramakrishna, Development of nanocomposites for bone grafting, Compos. Sci. Technol. 65 (2005) 2385–2406, http://dx.doi.org/10.1016/j.compscitech.2005.07.022.

[11] R. Puxkandl, I. Zizak, O. Paris, J. Keckes, W. Tesch, S. Bernstorff, P. Purslow, P. Fratzl, Viscoelastic properties of collagen: synchrotron radiation investigations and structural model, Philos. Trans. R. Soc. B Biol. Sci. 357 (2002) 191–197, http://dx.doi.org/10.1098/rstb.2001.1033.

[12] R. Kane, P.X. Ma, Mimicking the nanostructure of bone matrix to regenerate bone, Mater. Today 16 (2013) 418–423, http://dx.doi.org/10.1016/j.mattod.2013.11.001.

[13] K.J. Burg, S. Porter, J.F. Kellam, Biomaterial developments for bone tissue engineering, Biomaterials 21 (2000) 2347–2359, http://dx.doi.org/10.1016/S0142-9612(00)00102-2.

[14] R. Parenteau-Bareil, R. Gauvin, F. Berthod, Collagen-based biomaterials for tissue engineering applications, Materials 3 (2010) 1863–1887, http://dx.doi.org/10.3390/ma3031863.

[15] C.M. Agrawal, J.L. Ong, M.R. Appleford, G. Mani, Introduction to Biomaterials: Basic Theory with Engineering Applications, Cambridge University Press, New York, NY, USA, 2013.

[16] K. Trabbic-Carlson, L.A. Setton, A. Chilkoti, Swelling and mechanical behaviors of chemically cross-linked hydrogels of elastin-like polypeptides, Biomacromolecules 4 (2003) 572–580, http://dx.doi.org/10.1021/bm025671z.

[17] J.C. Rodríguez-Cabello, L. Martín, A. Girotti, C. García-Arévalo, F.J. Arias, M. Alonso, Emerging applications of multifunctional elastin-like recombinamers, Nanomedicine 6 (2011) 111–122, http://dx.doi.org/10.2217/nnm.10.141.

[18] S.S. Amruthwar, A.V. Janorkar, In vitro evaluation of elastin-like polypeptide-collagen composite scaffold for bone tissue engineering, Dent. Mater. 29 (2013) 211–220, http://dx.doi.org/10.1016/j.dental.2012.10.003.

[19] N. Ozturk, A. Girotti, G.T. Kose, J.C. Rodríguez-Cabello, V. Hasirci, Dynamic cell culturing and its application to micropatterned, elastin-like protein-modified poly(N-isopropylacrylamide) scaffolds, Biomaterials 30 (2009) 5417–5426, http://dx.doi.org/10.1016/j.biomaterials.2009.06.044.

[20] E. Salvagni, G. Berguig, E. Engel, J.C. Rodriguez-Cabello, G. Coullerez, M. Textor, J.A. Planell, F.J. Gil, C. Aparicio, A bioactive elastin-like recombinamer reduces unspecific protein adsorption and enhances cell response on titanium surfaces, Colloids Surf. B Biointerfaces 114 (2014) 225–233, http://dx.doi.org/10.1016/j.colsurfb.2013.10.008.

[21] S. Prieto, A. Shkilnyy, C. Rumplasch, A. Ribeiro, F.J. Arias, J.C. Rodríguez-Cabello, A. Taubert, Biomimetic calcium phosphate mineralization with multifunctional elastin-like recombinamers, Biomacromolecules 12 (2011) 1480–1486, http://dx.doi.org/10.1021/bm200287c.

[22] P.A. Raj, M. Johnsson, M.J. Levine, G.H. Nancollas, Salivary statherin: dependence on sequence, charge, hydrogen bonding potency, and helical conformation for adsorption to hydroxyapatite and inhibition of mineralization, J. Biol. Chem. 267 (1992) 5968–5976.

[23] D. Carnelli, P. Vena, M. Dao, C. Ortiz, R. Contro, Orientation and size-dependent mechanical modulation within individual secondary osteons in cortical bone tissue, J. R. Soc. Interface 10 (2013) 1–12, http://dx.doi.org/10.1098/rsif.2012.0953.

[24] J.S. Barbosa, R.R. Costa, A.M. Testera, M. Alonso, J.C. Rodríguez-Cabello, J.F. Mano, Multi-layered films containing a biomimetic stimuli-responsive recombinant protein, Nanoscale Res. Lett. 4 (2009) 1247–1253, http://dx.doi.org/10.1007/s11671-009-9388-5.

[25] H. Kenar, A. Kocabas, A. Aydinli, V. Hasirci, Chemical and topographical modification of PHBV surface to promote osteoblast alignment and confinement, J. Biomed. Mater. Res. A 85 (2008) 1001–1010, http://dx.doi.org/10.1002/jbm.a.31638.

[26] E. Sayin, E. Türker Baran, V. Hasirci, Osteogenic differentiation of adipose derived stem cells on high and low aspect ratio micropatterns, J. Biomater. Sci. Polym. Ed. 5063 (2015) 1–44, http://dx.doi.org/10.1080/09205063.2015.1100494.

[27] M.P. Francis, P.C. Sachs, L.W. Elmore, S.E. Holt, Isolating adipose-derived mesenchymal stem cells from lipoaspirate blood and saline fraction, Organogenesis 6 (2010) 11–14. http://www.pubmedcentral.nih.gov/articlerender.fcgi?artid=2861738&tool=pmcentrez&rendertype=abstract.

[28] G.M. Cooper, The Cell - A Molecular Approach, second ed., Sinauer Associates, Sunderland (MA), 2000 citeulike-article-id:10266975.

[29] I. Sakurada, Polyvinyl Alcohol Fibers, CRC Press, 1985.

[30] Q. Lu, B. Zhang, M. Li, B. Zuo, D.L. Kaplan, Y. Huang, H. Zhu, Degradation

mechanism and control of silk fibroin, Biomacromolecules 12 (2011) 1080–1086, http://dx.doi.org/10.1021/bm101422j.
[31] Q. Lv, K. Hu, Q. Feng, F. Cui, Fibroin/collagen hybrid hydrogels with cross-linking method: preparation, properties, and cytocompatibility, J. Biomed. Mater. Res. Part A 84 (1) (2008) 198–207, http://dx.doi.org/10.1002/jbm.a.31366.
[32] S. Das, F. Pati, Y.J. Choi, G. Rijal, J.H. Shim, S.W. Kim, A.R. Ray, D.W. Cho, S. Ghosh, Bioprintable, cell-laden silk fibroin-gelatin hydrogel supporting multilineage differentiation of stem cells for fabrication of three-dimensional tissue constructs, Acta Biomater. 11 (2015) 233–246, http://dx.doi.org/10.1016/j.actbio.2014.09.023.
[33] M.D. Shoulders, R.T. Raines, Collagen structure and stability, Annu. Rev. Biochem. 78 (2009) 929–958, http://dx.doi.org/10.1146/annurev.biochem.77.032207.120833.
[34] C.R. Wheeless, J.A. Nunley, J.R. Urbaniak, in: D.U.M.C.D. of O. Surgery, Wheeless' Textbook of Orthopaedics, 2016.
[35] Y.J. Ryu, T.J. Cho, D.S. Lee, J.Y. Choi, J. Cho, Phenotypic characterization and In vivo localization of human adipose-derived mesenchymal stem cells, Mol. Cells 35 (2013) 557–564, http://dx.doi.org/10.1007/s10059-013-0112-z.
[36] S.F. El-Amin, E. Botchwey, R. Tuli, M.D. Kofron, A. Mesfin, S. Sethuraman, R.S. Tuan, C.T. Laurencin, Human osteoblast cells: isolation, characterization, and growth on polymers for musculoskeletal tissue engineering, J. Biomed. Mater. Res. Part A 76 (2006) 439–449, http://dx.doi.org/10.1002/jbm.a.30411.
[37] J.E. Aubin, F. Lui, L. Malaval, A.K. Gupta, Osteoblast and chondroblast differentiation, Bone 17 (1995), http://dx.doi.org/10.1016/8756-3282(95)00183-E.
[38] M.J. Coelho, M.H. Fernandes, Human bone cell cultures in biocompatibility testing. Part II: effect of ascorbic acid, β-glycerophosphate and dexamethasone on osteoblastic differentiation, Biomaterials 21 (2000) 1095–1102, http://dx.doi.org/10.1016/S0142-9612(99)00192-1.
[39] S.I. Roohani-Esfahani, Z.F. Lu, J.J. Li, R. Ellis-Behnke, D.L. Kaplan, H. Zreiqat, Effect of self-assembled nanofibrous silk/polycaprolactone layer on the osteoconductivity and mechanical properties of biphasic calcium phosphate scaffolds, Acta Biomater. 8 (2012) 302–312, http://dx.doi.org/10.1016/j.actbio.2011.10.009.
[40] S. Gronthos, K. Stewart, S.E. Graves, S. Hay, P.J. Simmons, Integrin expression and function on human, J. Bone Min. Res. 12 (1997) 1189–1197, http://dx.doi.org/10.1359/jbmr.1997.12.8.1189.
[41] J.R. Mauney, T. Nguyen, K. Gillen, C. Kirker-Head, J.M. Gimble, D.L. Kaplan, Engineering adipose-like tissue *in vitro* and *in vivo* utilizing human bone marrow and adipose-derived mesenchymal stem cells with silk fibroin 3D scaffolds, Biomaterials 28 (2007) 5280–5290, http://dx.doi.org/10.1016/j.biomaterials.2007.08.017.
[42] F. Causa, P.A. Netti, L. Ambrosio, G. Ciapetti, N. Baldini, S. Pagani, D. Martini, A. Giunti, Poly-epsilon-caprolactone/hydroxyapatite composites for bone regeneration: *in vitro* characterization and human osteoblast response, J. Biomed. Mater. Res. Part A 76 (2006) 151–162, http://dx.doi.org/10.1002/jbm.a.30528.
[43] H. Kenar, G.T. Köse, V. Hasirci, Tissue engineering of bone on micropatterned biodegradable polyester films, Biomaterials 27 (2006) 885–895, http://dx.doi.org/10.1016/j.biomaterials.2005.07.001.
[44] N.E. Vrana, A. Elsheikh, N. Builles, O. Damour, V. Hasirci, Effect of human corneal keratocytes and retinal pigment epithelial cells on the mechanical properties of micropatterned collagen films, Biomaterials 28 (2007) 4303–4310, http://dx.doi.org/10.1016/j.biomaterials.2007.06.013.
[45] P. Zorlutuna, N. Builles, O. Damour, A. Elsheikh, V. Hasirci, Influence of keratocytes and retinal pigment epithelial cells on the mechanical properties of polyester-based tissue engineering micropatterned films, Biomaterials 28 (2007) 3489–3496, http://dx.doi.org/10.1016/j.biomaterials.2007.04.013.
[46] N. Ozturk, A. Girotti, G.T. Kose, J.C. Rodríguez-Cabello, V. Hasirci, Dynamic cell culturing and its application to micropatterned, elastin-like protein-modified poly(N-isopropylacrylamide) scaffolds, Biomaterials 30 (2009) 5417–5426, http://dx.doi.org/10.1016/j.biomaterials.2009.06.044.
[47] M.J.P. Biggs, R.G. Richards, S. McFarlane, C.D.W. Wilkinson, R.O.C. Oreffo, M.J. Dalby, Adhesion formation of primary human osteoblasts and the functional response of mesenchymal stem cells to 330nm deep microgrooves, J. R. Soc. Interface 5 (2008) 1231–1242, http://dx.doi.org/10.1098/rsif.2008.0035.
[48] T. Kim, S. Shah, L. Yang, P.T. Yin, K. Hossain, B. Conley, J. Choi, K. Lee, Controlling differentiation of adipose-derived stem cells using combinatorial graphene hybrid-pattern arrays, ACS Nano 9 (2015) 3780–3790, http://dx.doi.org/10.1021/nn5066028.
[49] S. Wang, M.J. Yaszemski, J.A. Gruetzmacher, L. Lu, Photo-crosslinked poly(ε-caprolactone fumarate) networks: roles of crystallinity and crosslinking density in determining mechanical properties, Polymer 49 (2008) 5692–5699, http://dx.doi.org/10.1016/j.polymer.2008.10.021.
[50] K. Hu, Biocompatible fibroin blended films with recombinant human-like collagen for hepatic tissue engineering, J. Bioact. Compat. Polym. 21 (2006) 23–37, http://dx.doi.org/10.1177/0883911506060455.
[51] E. Tejeda-Montes, A. Klymov, M.R. Nejadnik, M. Alonso, J.C. Rodriguez-Cabello, X.F. Walboomers, A. Mata, Mineralization and bone regeneration using a bioactive elastin-like recombinamer membrane, Biomaterials 35 (2014) 8339–8347, http://dx.doi.org/10.1016/j.biomaterials.2014.05.095.
[52] L. Rifas, L.R. Halstead, W.A. Peck, L.V. Avioli, H.G. Welgus, Human osteoblasts *in vitro* secrete tissue inhibitor of metalloproteinases and gelatinase but not interstitial collagenase as major cellular products, J. Clin. Investig. 84 (1989) 686–694, http://dx.doi.org/10.1172/JCI114216.
[53] H. Egusa, K. Iida, M. Kobayashi, T.Y. Lin, M. Zhu, P.A. Zuk, C.J. Wang, D.K. Thakor, M.H. Hedrick, I. Nishimura, Downregulation of extracellular matrix-related gene clusters during osteogenic differentiation of human bone marrow- and adipose tissue-derived stromal cells, Tissue Eng. 13 (2007) 2589–2600, http://dx.doi.org/10.1089/ten.2007.0080.
[54] A. Ascenzi, E. Bonucci, The tensile properties of single osteons, Anat. Rec. 158 (1967) 375–386, http://dx.doi.org/10.1002/ar.1091580403.